Sensitivity Analysis for Frequency Regulation in a Two-area Power System

Julian Patino *‡, Felipe Valencia **, Jairo Espinosa ***

*Departmento de Ingeniería Eléctrica, Facultad de Ingeniería y Arquitectura, Universidad Nacional de Colombia, Manizales, Colombia

**Solar Energy Research Center-SERC Chile, Faculty of Mathematical and Physical Sciences, University of Chile, Santiago, Chile

***Departmento Ingeniería Eléctrica y Automática, Facultad de Minas, Universidad Nacional de Colombia, Medellín, Colombia

(japatin0@unal.edu.co, felipe.valencia@sercchile.cl, jespinov@unal.edu.co)

‡ Corresponding Author; Julian Patino, Carrera 80 No 65-223, Medellín, Colombia,

Tel: +57(4) 425 52 60, Fax: +57(4) 425 52 60, japatin0@unal.edu.co

Received: 17.11.2016 Accepted:02.01.2017

Abstract- In recent years, the integration level of renewable energy sources into the grid system has grown considerably. In the near future, renewable-based power is expected to be comparable to the conventional power generation systems. Nevertheless, the variations in renewable power can induce negative effects on power systems, such as frequency disturbances. This paper presents a study of the sensitivity functions for system frequency to power changes produced by renewable energy sources. Transfer functions are analyzed using Bode plots. The results reveal that there is a region where the impacts of the harmonic contents of the power variations cause larger impacts on both the frequency and the total transferred power of a given control area.

Keywords Renewable energy systems; power system control; frequency regulation; sensitivity analysis; Bode plots.

1. Introduction

The worldwide penetration of renewable energy sources (RES) for generation of electricity is increasing and trending up [1]. Aspects such as humanity ever growing need for electric energy, the limited reserves of fossil fuels and the environmental concerns over greenhouse-gases impulse a continuous development of these new generation systems. Even if some characteristics such as reliability, controllability and availability of the power produced from RES sources are radically different with respect to conventional power generation [2]. Additionally, because renewable resources sometimes are unpredictable, very variable and location-dependent, their generated power output may present significant fluctuations over time [3]. Large penetration of renewable energy cause many different impacts in the operation and control of power systems [3]–[5]; frequency performance constitutes one of the main important issues and has attracted considerable research interest [3], [6], [7].

In power systems, rotational speed of the synchronous machines determines system frequency. Frequency is a parameter that indicates the balance between power generation and load demand. In presence of renewable energy sources, the power fluctuations produced may cause unbalances in the load – generation relationship, therefore resulting in frequency deviations from the operational standard. Control systems are in place for facing these situations: variations in operational speed of synchronous units are attenuated by machine inertia, and primary (Load Frequency Control) and secondary (Automatic Generation Control) control schemes will restore system frequency to the standard value. However, these control systems were usually designed for the operation of conventional units. There is a need to study the effects of renewable energy sources over the power system frequency and its components. As the most popular RES around the world, frequency control requirements and methods have been studied for solar photovoltaic systems [6], [8] and more extensively for wind generation [6], [9], [10] (the latter reference presents a

complete summary of grid requirements and control strategies).

This paper focuses on the analysis of the effects of active power variations that could be caused from renewable energy sources in the system frequency. Sensitivity functions are established using linearized models and transfer function representations for the system components, and Bode Diagrams are used as the analysis tool. A first approximation for the same methodology can be found in [11]. Results are illustrated through simulation of a multi-area system. Although Bode Diagrams were previously employed for studying wind power impacts in power systems [12], [13], those works only deal with isolated one-area systems. Also, transfer functions for control system frequency components are developed in [14], [15]. However, they are used to determine the system sensitivities to machine parameters like inertia, damping and speed droop, and not for the analysis of the effects of renewable energy sources.

The paper is organized as follows. The first part presents a brief description of frequency regulation in power systems, indicating the main stages of the regulation schemes. Later, the classical model for frequency regulation in power systems is presented in a two-area configuration. Sensitivity functions with respect to load disturbances are obtained for the two-area case and Bode plots for each function are calculated. The results of the Bode diagrams are evaluated through the application of a wind energy source acting as disturbance for the frequency regulation scheme in one of the areas. At the end, there is a discussion of results and some conclusions.

2. Frequency Regulation in Power Systems

2.1. Description

The effects of large disturbances in electrical power systems are notorious, and may cause variations in both active and reactive power. Usually, the loss of the equilibria between demanded and generated reactive power leads to voltage modifications; unbalances in generated and demanded active power result in frequency changes. Each generator is affected by these unbalances in different ways according to its role in the system and its own parameters and configuration. As mentioned in [6], "a large frequency deviation can damage equipment, degrade load performance, cause the transmission lines to be overloaded, and can interfere with system protection schemes, ultimately leading to an unstable condition for the power system."

The automatic system for frequency regulation is composed by two main parts: primary and secondary control. Tertiary control, another stage consisting of the release of control reserves after a disturbance, is not considered a specific part of frequency regulation [16]. This is because the use of those control reserves, after a manually activated process, is more related to the energy production process according to the generation scheduling (dispatch).

Primary control is related to locally executed control actions (plant-level in generation units) based in the reference values for frequency and generated power. The operating values of both of those variables can be measured on-site. Deviations from reference values will result in a control signal that will action valves, gates, servomotors and other elements in the turbine-generator group, in order to produce the required active power. In primary frequency control the main task is the fast frequency restoration to appropriate operational levels, although small deviations can be attenuated under normal conditions. However, there is a remaining steady-state error from frequency reference values because the control action only involves a proportional gain. Primary control is shared by all the generating units regardless of the disturbance location.

Secondary frequency regulation, or Load Frequency Control (LFC), has to restore system frequency for deviations large enough to escape the primary control action. In LFC, the reference values for the generation of active power are adjusted to eliminate the remaining steady-state error in system frequency. Besides this, secondary control also must react to variations in the transferred power flows exchanged by the control area; these flows can change due to active power unbalances and primary control actions. Typically, secondary control is designed to response only to local area disturbances. When this control loop performs in a fully automated way, the scheme is denominated Automatic Generation Control (AGC).

2.2. Modelling of frequency regulation

As frequency in an electric power system is directly related with rotational speed of generation units, frequency regulation can be transformed into a speed control issue for generators. Frequency variation in power systems can be represented by the so called swing equation [17]:

$$J\frac{d\omega}{dt} = T_m - T_e \tag{1}$$

In equation (1), J is the merged inertia moment for turbine and generator [kg m^2], ω the rotor angular speed [rad/s], t is time [s], T_m and T_e the mechanical, and electromagnetic torque, respectively [N m]. There are many ways to write the swing equation; after some mathematical manipulations, and using Laplace transformation, we can obtain the following expression:

$$\Delta P_m(s) - \Delta P_L(s) = 2Hs\Delta f(s) + D\Delta f(s). \tag{2}$$

In equation (2), Δf represents the normalized frequency deviation [p.u], ΔP_m the variation in machine mechanical power [p.u], ΔP_L the change in load demanded power [p.u], H is the corresponding inertia constant per machine power rating [s], and D load damping constant. Equation (2) represents frequency variations in a synchronous machine. Variations in the mechanical power ΔP_m can be represented through the use of models for the machine speed governor and turbine. Several models have been proposed for modeling the dynamic characteristics of turbine and speed governor in power system frequency analysis and controller design [17]. Often, first order representations are used for conventional hydro and thermal units; the proportional action of primary control is applied through the droop characteristic of each generator (denoted by R).

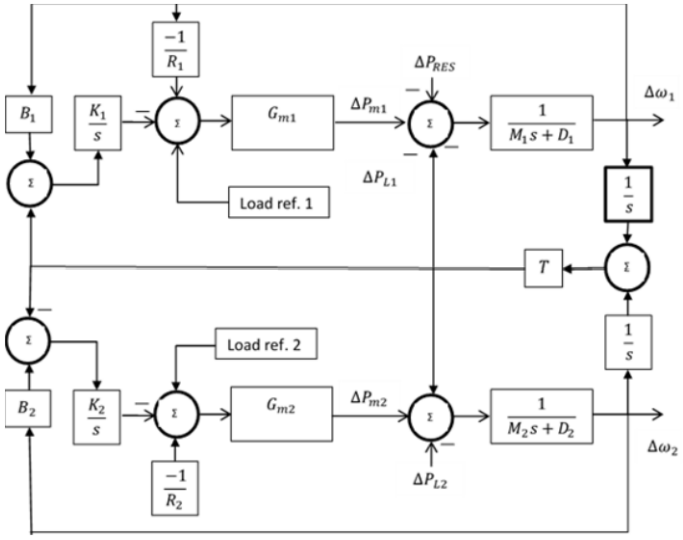

Fig. 1. Block diagram of the two area system model for frequency response analysis. (Based on [17]).

In Fig. 1 a block diagram representation of a two area system is depicted. There, $G_m(s)$ denotes the transfer function for the turbine-governor group, $K(s) = k_i/s$ is the integral secondary controller, the bias factor for each area is $\beta_i = 1/R_i + D_i$, and T is constant defined as the synchronizing power coefficient [17]. Also, $M = 2H$, $\omega = 2\pi f$, and the interchanged power flow between areas is denoted by ΔP_{12}.The blocks marked as load ref represent the changes in machine power set-points, and are assumed to be at zero value.

3. Sensitivity Analysis for Frequency Regulation

In order to describe the relationships between area frequencies and the applied disturbances, the transfer functions need to be expressed. From Fig. 1, the following relationships can be extracted:

$$\Delta P_{12}(s) = \frac{2\pi}{s} T\left(\Delta f_1(s) - \Delta f_2(s)\right) \tag{3}$$

$$\Delta f_1(s) = G_1(s)[A_1(s)G_{m1}(s)\Delta f_1(s) + F_1(s)\Delta P_{12}(s) - \Delta P_{L1}(s)]$$

$$\Delta f_2(s) = G_2(s)[A_2(s)G_{m2}(s)\Delta f_2(s) - F_2(s)\Delta P_{12}(s) - \Delta P_{L2}(s)]$$

Table 1. Appearance properties of accepted manuscripts

Parameter	*Area 1*	*Area 2*
Mi	10	8
Di	0.6	0.9
Tgi	0.2 s	0.2 s
Tchi	0.5 s	0.5 s
Ri	1/20	1/20
Ki	-0.3	-0.3
βi	20.6	16.9
T	2	2
F_0	60 Hz	60 Hz

In the previous set of equations, for $i = \{1,2\}$:

$$G_i(s) = \frac{1}{2H_i s + D_i} \tag{4}$$

$$A_i(s) = \left(\beta_i \frac{k_i}{s} - \frac{1}{R_i}\right)$$

$$F_i(s) = \left(\frac{k_i}{s} G_{mi}(s) - 1\right)$$

The system composed for Equations (3) and (4) is solved for $\Delta f_1(s)$, $\Delta f_2(s)$ and $\Delta P_{12}(s)$ as functions of load disturbances $\Delta P_{L1}(s)$ and $\Delta P_{L2}(s)$. Assuming one of the load disturbances as equal to zero, the transfer functions with respect of the other can be established. Therefore, for $\Delta P_{L2}(s) = 0$, the transfer function between both area frequencies and the transferred power with respect to $\Delta P_{L1}(s)$ are found and denoted by:

$$G_{f1,PL1}(s) = \frac{\Delta f_1(s)}{\Delta P_{L1}(s)} \tag{5}$$

$$G_{f2,PL1}(s) = \frac{\Delta f_2(s)}{\Delta P_{L1}(s)}$$

$$G_{P12,PL1}(s) = \frac{\Delta P_{12}(s)}{\Delta P_{L1}(s)}$$

Conversely making $\Delta P_{L1}(s) = 0$, and in a similar notation as above, transfer functions $G_{f1,PL2}(s)$, $G_{f2,PL2}(s)$ and $G_{P12,PL2}(s)$ can be easily obtained. For the full expression of the transfer functions, the system machines for both areas are going to be considered as thermal units, modeled as shown in equation (6). Parameters T_{gi} and T_{chi} are time constants in seconds.

$$G_{mi} = \left(\frac{1}{T_{gi}s+1}\right)\left(\frac{1}{T_{chi}s+1}\right), \; for \;\; i = 1,2 \tag{6}$$

Bode plots are employed for the study of the transfer functions in the group of equations (5). As defined in [18], "Bode plots are graphs of the steady-state response of stable, continuous- time Linear Time Invariant systems for sinusoidal inputs, plotted as change in magnitude and phase versus frequency." Bode plots can be seen as a visual representation of a system behavior, and they represent a very useful tool in linear control theory.

In order to examine the behavior of the transfer functions, and depict the Bode plots, computer simulations are performed using the parameters described in Table 1.

3.1. Sensitivity analysis with Bode Plots

As shown in Table 1, both areas have very similar parameter values, and the transferred power flows from area 1 to area 2. Figure 2 shows per-unit magnitude Bode plots for $G_{f1,PL1}(s)$ and $G_{f2,PL1}(s)$. For most of the spectrum both plots present responses with an attenuating behavior. This means that the low frequency power fluctuations are attenuated by AGC. In both cases, the high frequency (values greater than 1 Hz) power variations are damped by generator inertia. According to Figure 2, area 2 frequency is much less sensitive to load disturbances in area 1; this is expected from the design requirements of secondary control. There is only a narrow band between 0.4 and 0.9 Hz where the magnitude of the disturbance effects in area 2 is greater than 0..02 per unit. The sensitivity region for area 1 frequency is bigger, from 0.01 to

1 Hz, with a maximum value of 0.25 per unit at 0.27 Hz. We can conclude that area 1 frequency is *more sensitive* to load variations in area 1, and disturbances with spectral content inside the previously highlighted zone could cause major effects to system frequency in area 1.

Figure 3 depicts the per unit Bode plot for $G_{P12,PL1}(s)$. Transferred power has a wider region of sensitivity to area 1 disturbances than the case of the frequency functions, with values ranging from 0.001 to 1 Hz. Signals with harmonic content inside of this region could cause disturbances in transferred power. Figure 3 also shows a maximum peak value of 0.25 in magnitude at the same frequency of $G_{f1,PL1}(s)$. There is no sensitivity for disturbances beyond 1 Hz, just like the case of frequencies of both areas.

3.2. System Response to disturbances with different spectral content

Results of sensitivity analysis are verified through simulation, by the application of different disturbance signals with spectral content inside the different identified regions.

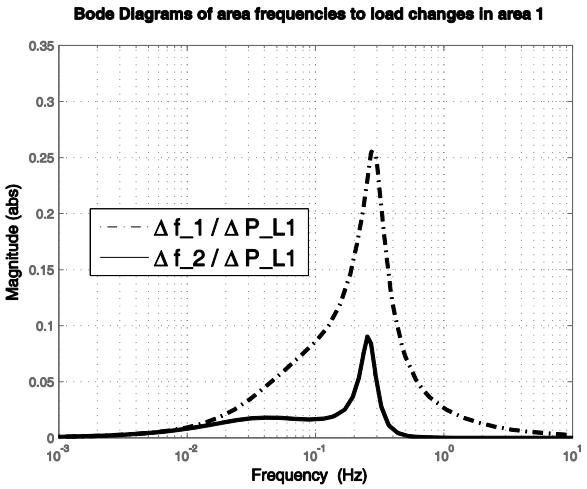

Fig. 2. Bode plots for $G_{f1,PL1}(s)$ (dotted line) and $G_{f2,PL1}(s)$ (solid line).

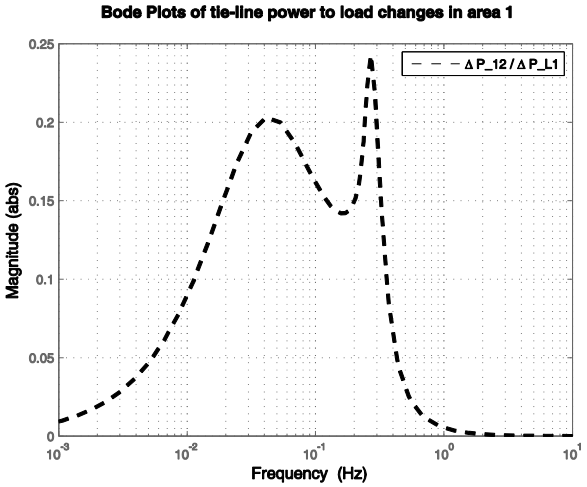

Fig. 3. Bode plot for $G_{P12,PL1}(s)$

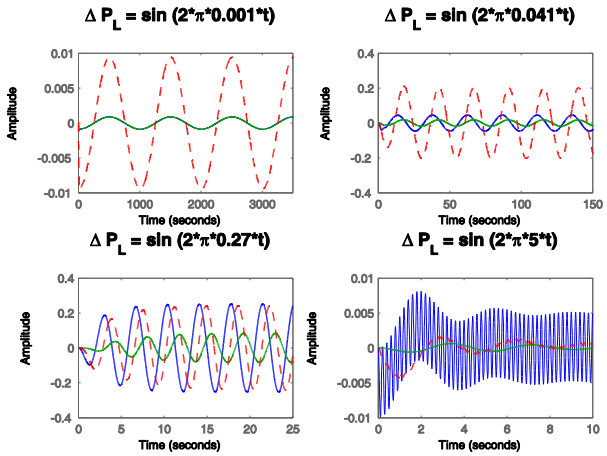

Fig. 4. Time responses of $G_{f1,PL1}(s)$ (blue), and $G_{f2,PL1}(s)$ (green) and $G_{P12,PL1}(s)$ (red) for different load disturbance signals.

The resulting plots are depicted in Fig. 4. Sine waves of different frequencies were applied as load disturbances in area 1, all of them having and unitary amplitude (per unit). Comments on every response are listed below:

- At first, the system response a sine with a frequency of 0.001 Hz shows activity only for the transfer function of the transferred power between areas ($G_{P12,PL1}(s)$); the response for both area frequencies are almost zero, and it is hard to separate each response in the resulting image.

- For a sine disturbance of 0.041 Hz, all the transfer functions have a response. However, both $G_{f1,PL1}(s)$ and $G_{f2,PL1}(s)$ signals have a magnitude of about 0.05 (per unit), and the amplitude for $G_{P12,PL1}(s)$ has and absolute value around 0.2 (per unit). This is expected from Fig. 3, as the transfer function of transferred power reaches its second maximum value at 0.041 Hz.

- As seen from figures 2 and 3, the maximum peak response for all the transfer functions is reached at 0.27 Hz. This is verified with a sine disturbance of this frequency value, showing an amplitude for $G_{f1,PL1}(s)$ of an absolute value of about 0.25 (per unit), just slightly bigger than the amplitude of $G_{P12,PL1}(s)$. Response for $G_{f2,PL1}(s)$ is also greater than the other cases, too.

- Finally, a sine load disturbance of 5 Hz is applied. For this frequency value, the $G_{f1,PL1}(s)$ response is bigger than the others, even when its magnitude oscillates around a maximum absolute amplitude of 0.005 (per unit). This is expected because the transfer functions $G_{f2,PL1}(s)$ and $G_{P12,PL1}(s)$ have almost zero amplitude for frequencies over 1 Hz.

This simple simulation illustrates the possible application of the results of the sensitivity analysis using Bode plots for predicting the frequency regulation performance to load disturbances. This could lead to the development of a useful tool for the assessment of system performance with renewable penetration, as shown in the next section.

4. System Response to Wind Power Disturbances

We are interested in the determination of the effects of renewable energy sources in power system frequency regulation. In these way, and continuing with the previously employed simulation scenario, let's assume that a wind farm is inserted in the generation mix of area 1. Using a wind profile obtained from the database of Virgin Islands (USA) [19] as the base for the source signal, we reproduce the generated power from a set of typical wind turbines, denoted by ΔP_W and shown in Figure 5. Data is obtained for a complete day and sampled by minute. For the sake of simulation, we assume a sampling frequency of 1 second.

Since the wind farm does not contribute to the frequency regulation schemes, its power variations are considered as load variations in the area, so it is assumed that $\Delta P_{L1} = \Delta P_W$. As we saw from the sensitivity analysis and the Bode plots from previous section, there are some regions where the load disturbances are more dangerous for the system. In order to know whether this signal ΔP_W belongs to these regions or not, we obtain the periodogram using the Fast Fourier Transform, as shown in Figure 5.

The main spectral content of ΔP_W is concentrated below 0.05 Hz; for these values, only the transferred power $\Delta P_{12}(s)$ could be affected for the spectral content of the signal. The spectral content at 0.27 Hz (frequency of maximum sensitivity) has a value of 0.0007123. Therefore, this mode does not represent a real threat for frequency regulation with the given wind power variations. The principal cause of concern for the frequency regulation is the amplitude of the variations in ΔP_W going over 0.3 [p.u] at some points. Any variation of about 30% of the rated area power will have consequences regardless the kind of generation involved (either conventional or renewable-based, or both).

4.1. Responses to wind power variations

Figures 7, 8 and 9 present the time responses for Δf_1, Δf_2 and ΔP_{12}, respectively, after the application of the signal ΔP_W as a load disturbance in area 1. As seen from ΔP_W in Fig. 5, the power generated from the wind farm under 500 seconds is almost zero; consequently, the transferred power and both time responses of the area frequencies remain almost unchanged for the same time interval. In total, the simulation lasts over 1400 seconds.

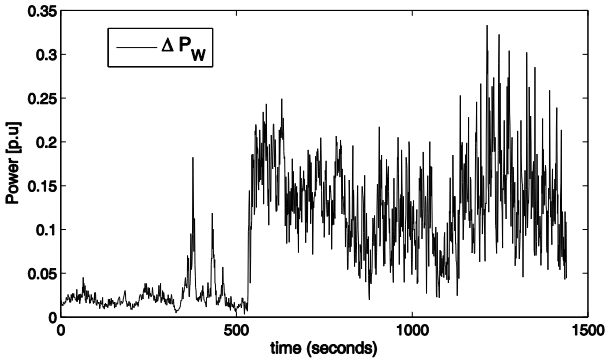

Fig. 5. Wind power fluctuations ΔP_W

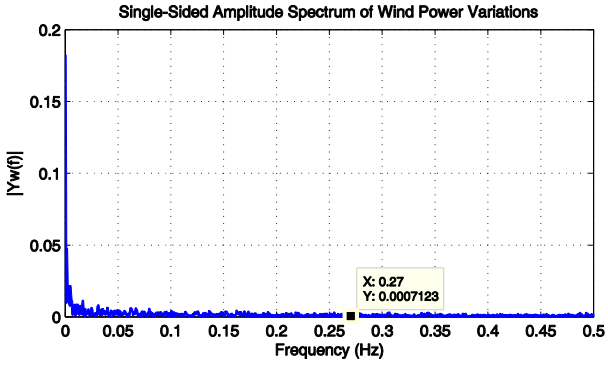

Fig. 6. Periodogram ΔP_W

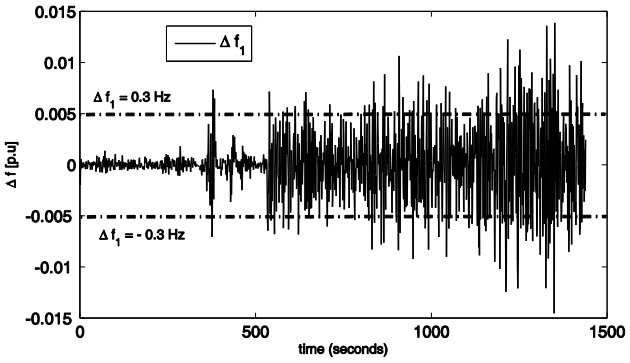

Fig. 7. Variations in area 1 frequency due to $\Delta P_{L1} = \Delta P_W$

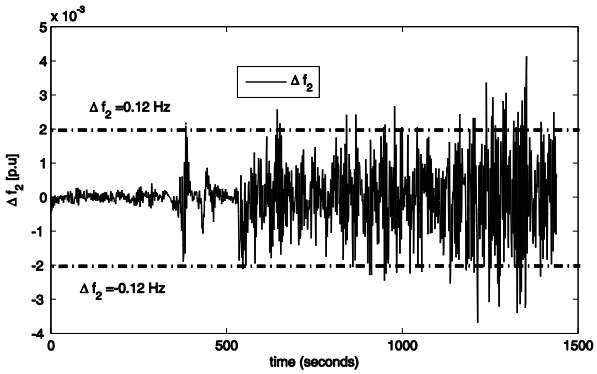

Fig. 8. Variations in area 1 frequency due to $\Delta P_{L1} = \Delta P_W$

The plots of frequency variations for area 1 and area 2 have a very similar behavior, differing almost exclusively in magnitude. In both Fig. 7 and Fig. 8, the magnitude of the frequency deviations is presented in *per-unit* system. In order to have a better grasp of the size of the variations, some limit deviations have been highlighted in both areas. The operating frequency of the simulation is 60 Hz. Therefore, regions involve variations with a maximum absolute value of 0.12 Hz for area 2 and 0.3 Hz for area 1. These limit values are intriguing because the trespassing of them could lead to penalties for the generation entity, depending on the grid code and the operation requirements [10].

The wind farm is located at area 1, acting as a load disturbance to the frequency regulation scheme. Usually, the parameters of the controllers in primary and secondary frequency control are tuned in such a way that disturbances do not propagate to the other areas. According to this fact, and the sensitivity analysis performed in previous sections, it is

somewhat straightforward that area 1 frequency (Δf_1) is more affected, reaching the mentioned values of 0.3 Hz o getting near them many times over the simulation. Also, as expected from the sensitivity analysis, values of Δf_2 are very low, only exceeding 0.12 Hz at the extreme values of wind power deviation. The average frequency deviations per-sample over the simulation were $\Delta f_{1,avg} = 0.1625\ Hz$, and $\Delta f_{2,avg} = 0.0455\ Hz$.

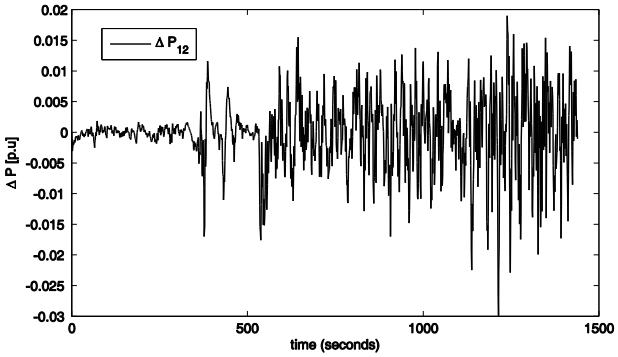

Fig. 9. Variations in transferred power due to $\Delta P_{L1} = \Delta P_W$

Fig. 9 demonstrates how transferred power time response has a similar behavior to the area frequency plots, even though it looks more disperse. The increased activity after 500 seconds can be attributed to the variations in wind power generation after the same time period. As the area 1 frequency starts to deviate from normal operation, transferred power also starts to oscillate to compensate for frequency variations. The average transferred power deviation per-sample over the simulation was $\Delta P_{12,avg} = 0.2876$ [p.u].

5. Conclusion

The use of Bode plots as analysis tool for the determination of the impacts of load disturbances in frequency regulation schemes shows that there are regions of major impact according to the disturbance spectral characteristics. The *a priori* knowledge of these sensible zones could lead to the identification of dangerous disturbances, and the development of compensation techniques that attenuate the adverse effects in advance. This will come in handy for the accommodation of renewable energy sources into the power systems, a task that could lead to disturbances in frequency regulations schemes, as it was observed the simulation of a wind farm in a two-area power system.

The increased penetration of renewable energy sources could also require call for the involvement of these kind of generation in frequency regulation tasks. In turn, given the new requirements and the different characteristics of renewable energy sources with respect to conventional units, this may result in the suggestion of different or additional control loops in for frequency regulation for maintaining a secure and stable network operation.

Acknowledgements

The work of Julian Patiño is being supported by Colciencias through the program "Convocatoria 528 - Convocatoria Nacional para Estudios de Doctorados en Colombia 2011".

References

[1] REN21, Ed., Renewables 2014 Global Status Report. Paris: REN21 Secretariat, 2014

[2] H. Bevrani, Intelligent automatic generation control. Boca Raton: CRC Press, 2011.

[3] C. L. DeMarco and C. A. Baone, "Chapter 29 - Control of Power Systems with High Penetration Variable Generation," in *Renewable Energy Integration*, L. E. Jones, Ed. Boston: Academic Press, 2014, pp. 369 – 379.

[4] I. J. Pérez-Arriaga, "Managing large scale penetration of intermittent renewables," MIT Energy Initiative Annual Symposium, Framework paper, Apr. 2011.

[5] T. R. Ayodele, A. A. Jimoh, J. L. Munda, and J. T. Agee, "Challenges of grid integration of wind power on power system grid integrity: A review," *Int. J. Renew. Energy Res.*, vol. 2, no. 4, pp. 618–626, 2012

[6] H. Bevrani, *Robust Power System Frequency Control*, 2nd ed. Springer, 2014

[7] S. K. Pandey, S. R. Mohanty, and N. Kishor, "A literature survey on load–frequency control for conventional and distribution generation power systems," *Renew. Sustain. Energy Rev.*, vol. 25, no. 0, pp. 318 – 334, 2013.

[8] C. Rahmann and A. Castillo, "Fast Frequency Response Capability of Photovoltaic Power Plants: The Necessity of New Grid Requirements and Definitions," *Energies*, vol. 7, no. 10, p. 6306, 2014.

[9] X. Yingcheng and T. Nengling, "Review of contribution to frequency control through variable speed wind turbine," *Renew. Energy*, vol. 36, no. 6, pp. 1671 – 1677, 2011.

[10] F. Díaz-González, M. Hau, A. Sumper, and O. Gomis-Bellmunt, "Participation of wind power plants in system frequency control: Review of grid code requirements and control methods," *Renew. Sustain. Energy Rev.*, vol. 34, no. 0, pp. 551 – 564, 2014.

[11] R. Horta, J. Espinosa, and J. Patino, "Frequency and voltage control of a power system with information about grid topology," in *Automatic Control (CCAC), 2015 IEEE 2nd Colombian Conference on*, 2015, pp. 1–6.

[12] W. Li, G. Joos, and C. Abbey, "Wind Power Impact on System Frequency Deviation and an ESS based Power Filtering Algorithm Solution," in *Power Systems Conference and Exposition, 2006. PSCE '06. 2006 IEEE PES*, 2006, pp. 2077–2084.

[13] C. Luo, H. G. Far, H. Banakar, P.-K. Keung, and B.-T. Ooi, "Estimation of Wind Penetration as Limited by Frequency Deviation," *Energy Convers. IEEE Trans. On*, vol. 22, no. 3, pp. 783–791, Sep. 2007.

[14] H. Huang and F. Li, "Sensitivity Analysis of Load-Damping Characteristic in Power System Frequency

Regulation," *Power Syst. IEEE Trans. On*, vol. 28, no. 2, pp. 1324–1335, May 2013.

[15] H. Huang and F. Li, "Sensitivity analysis of load-damping, generator inertia and governor speed characteristics in hydraulic power system frequency regulation," in *Power Engineering Conference (AUPEC), 2014 Australasian Universities*, 2014, pp. 1–6.

[16] G. Andersson, "Dynamics and Control of Electric Power Systems." EEH - Power Systems Laboratory, ETH Zurich, Feb-2012.

[17] P. Kundur, Power System Stability and Control. McGraw-Hill Professional, 1994.

[18] Z. Z. Karu, *Signals and systems made ridiculously simple*. Cambridge, MA: ZiZi Press, 1995.

[19] Roberts, O. and Andreas, A., "United States Virgin Islands: St. Thomas (Bovoni) & St. Croix (Longford)." NREL-DATA (National Renewable Energy Laboratory - Data (NREL-DATA), Golden, CO (United States)), 1997